PFOS-induced thyroid hormone system disrupted rats display organ-specific changes in their transcriptomes

Nichlas Davidsen, Louise Ramhøj, Claus Asger Lykkebo, Indusha Kugathas, Rikke Poulsen, Anna Kjerstine Rosenmai, Bertrand Evrard, Thomas A. Darde, Marta Axelstad, Martin Iain Bahl, et al.

PFOS-induced thyroid hormone system disrupted rats display organ-specific changes in their transcriptomes

Davidsen, Nichlas; Ramhøj, Louise; Lykkebo, Claus Asger; Kugathas, Indusha; Poulsen, Rikke; Rosenmai, Anna Kjerstine; Evrard, Bertrand; Darde, Thomas A.; Axelstad, Marta; Bahl, Martin Iain

Total number of authors:
14

Published in:
Environmental Pollution

Link to article, DOI:
10.1016/j.envpol.2022.119340

Publication date:
2022

Document Version
Publisher's PDF, also known as Version of record

Environmental Pollution 305 (2022) 119340

Contents lists available at ScienceDirect

Environmental Pollution

journal homepage: www.elsevier.com/locate/envpol

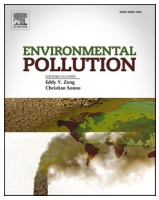

PFOS-induced thyroid hormone system disrupted rats display organ-specific changes in their transcriptomes☆

Nichlas Davidsen [a], Louise Ramhøj [a], Claus Asger Lykkebo [a], Indusha Kugathas [b], Rikke Poulsen [c], Anna Kjerstine Rosenmai [a], Bertrand Evrard [b], Thomas A. Darde [d], Marta Axelstad [a], Martin Iain Bahl [a], Martin Hansen [c], Frederic Chalmel [b], Tine Rask Licht [a], Terje Svingen [a,*]

[a] National Food Institute, Technical University of Denmark, Kgs. Lyngby, DK-2800, Denmark
[b] Univ Rennes, Inserm, EHESP, Irset (Institut de Recherche en Santé, Environnement et Travail), UMR_S 1085, F-35000, Rennes, France
[c] Department of Environmental Science, Aarhus University, Roskilde, DK-4000, Denmark
[d] SciLicium, Rennes, France

ARTICLE INFO

Keywords:
PFOS
Thyroid hormone
Transcriptomics
Vancomycin
Endocrine disrupting chemicals
Perfluorooctane sulfonate
PFAS
Perfluoroalkyl
Thyroid
HPT-axis

ABSTRACT

Perfluorooctanesulfonic acid (PFOS) is a persistent anthropogenic chemical that can affect the thyroid hormone system in humans and animals. In adults, thyroid hormones (THs) are regulated by the hypothalamic-pituitary-thyroid (HPT) axis, but also by organs such as the liver and potentially the gut microbiota. PFOS and other xenobiotics can therefore disrupt the TH system at various locations and through different mechanisms. To start addressing this, we exposed adult male rats to 3 mg PFOS/kg/day for 7 days and analysed effects on multiple organs and pathways simultaneously by transcriptomics. This included four primary organs involved in TH regulation, namely hypothalamus, pituitary, thyroid, and liver. To investigate a potential role of the gut microbiota in thyroid hormone regulation, two additional groups of animals were dosed with the antibiotic vancomycin (8 mg/kg/day), either with or without PFOS. PFOS exposure decreased thyroxine (T4) and triiodothyronine (T3) without affecting thyroid stimulating hormone (TSH), resembling a state of hypothyroxinemia. PFOS exposure resulted in 50 differentially expressed genes (DEGs) in the hypothalamus, 68 DEGs in the pituitary, 71 DEGs in the thyroid, and 181 DEGs in the liver. A concomitant compromised gut microbiota did not significantly change effects of PFOS exposure. Organ-specific DEGs did not align with TH regulating genes; however, genes associated with vesicle transport and neuronal signaling were affected in the hypothalamus, and phase I and phase II metabolism in the liver. This suggests that a decrease in systemic TH levels may activate the expression of factors altering trafficking, metabolism and excretion of TH. At the transcriptional level, little evidence suggests that the pituitary or thyroid gland is involved in PFOS-induced TH system disruption.

1. Introduction

Per- and polyfluoroalkyl substances (PFASs) are synthetic chemicals that are highly resistant to degradation. They are persistent in the environment and have long half-lives in humans (Olsen et al., 2007), properties that have lead to restrictions to the use of some PFASs over time (UNEP, 2008). However, people are still exposed through foods, water, dust, clothing, and other materials treated with PFASs (Sunderland et al., 2019). Perfluorooctanesulfonic acid (PFOS) is one legacy PFAS which has been shown to cause various health effects in animals and humans.

Both human and animal studies have linked PFOS exposure to TH system disruption (Coperchini et al., 2021, 2017; Fenton et al., 2021; Lee and Choi, 2017; Schrenk et al., 2020). Depending on the model system, various mechanisms by which PFOS could cause TH system disruption have been suggested. They include inhibition of the sodium/iodide symporter (NIS), disrupted thyroglobulin synthesis, altered thyroperoxidase (TPO) function, or increased TH excretion through liver enzyme induction and displacement of TH from transthyretin (TTR) (Coperchini et al., 2021; Dong et al., 2016; Ren et al., 2016; Weiss et al., 2009; Yu et al., 2009).

In rats, PFOS exposure reduces serum T4 and T3 levels, but typically

☆ This paper has been recommended for acceptance by Dr Jiayin Dai.

* Corresponding author.
E-mail address: tesv@food.dtu.dk (T. Svingen).

https://doi.org/10.1016/j.envpol.2022.119340
Received 10 February 2022; Received in revised form 14 April 2022; Accepted 18 April 2022
Available online 20 April 2022

does not activate the HPT axis by increasing TSH secretion. This hypothyroxinemia-like effect pattern of low THs and unaffected TSH has been observed in numerous animal studies of PFOS (Chang et al., 2008; Lau et al., 2003; Luebker et al., 2005; Thibodeaux et al., 2003; Yu et al., 2009), as well as for other environmental chemicals such as polybrominated diphenyl ethers (PBDEs), polychlorinated biphenyls (PCBs), triclosan and 3-methylcholanthrene (Bansal et al., 2014; Farmer et al., 2018; Goldey et al., 1995; Klaassen and Hood, 2001; Kodavanti et al., 2010; Liu et al., 1995; Louis et al., 2017). Yet, how these effects arises remain unclear (Gilbert et al., 2020).

Another point to consider with respect to PFOS exposure is the gut microbiota. The intestinal microbiota can affect TH metabolism by interfering with iodine uptake, as well as degradation and enterohepatic cycling of TH (Fröhlich and Wahl, 2019). In rats, an altered microbiota can lead to changes in serum TH levels, as well as TH excretion (de Herder et al., 1989). The microbiota also plays a role in the intestinal cycling of TH destined for excretion (de Herder et al., 1989; van der Spek et al., 2017) and PFASs are known to go through enterohepatic cycling in both humans and rats (Johnson et al., 1984; Zhao et al., 2017). Therefore, the composition of the gut microbiota could potentially impact how PFOS exposure disrupts the TH system.

With this complex, multi-organ system being affected by PFOS exposure, it is challenging to decipher exactly how PFOS causes changes to the TH system and resulting downstream adverse effect outcomes. To start addressing this, we performed transcriptomics analysis on several organs of the TH system to get a first glance at how TH system disruptors can affect several target organs, either directly or indirectly. By superimposing transcriptomics data on systemic TH profiles, potential targets for further in-depth analysis were identified. In addition, we included a PFOS exposure group where the gut microbiota was altered by vancomycin treatment, which could potentially reveal another level of complexity that needs to be accounted for when evaluating the potential risks of PFOS exposure. Notably, the study design does not allow for the decoupling of transcriptional changes occurring through a disrupted TH system versus effects mediated directly by PFOS in target tissues. Nevertheless, with this caveat in mind, the study design will offer insight into PFOS toxicity at the transcript level regardless of modality and provide a reference data source to compare future studies, including rats where the TH system has been disrupted by other means, and hence allowing for the early deciphering of TH-mediated effects at the organ level.

2. Materials & methods

2.1. Animal study

The study included 48 male Sprague-Dawley rat pups from timemated dams (Crl:CD(SD)), purchased from Charles River Europe (distributed by SCANBUR, Denmark). Male offspring were randomized and weaned for pairwise housing in cages at postnatal day (PD) 24. The rats were then semi-randomly distributed (according to weight) into 4 experimental groups until the end of the experiment (PD63). The 4 exposure groups were (n = 12/group): i) control (corn oil; Sigma Aldrich, MA, USA), ii) 8 mg Vancomycin hydrochloride/kg bw/day (CAS: 1404-93-9, lot# LRAC0718, Sigma Aldrich), iii) 3 mg heptadecafluoro-octanesulfonic acid potassium salt (PFOS)/kg bw/day (purity ≥98%, CAS: 2795-39-3, lot# BCCC4690, Merck), and iv) 8 mg Vancomycin (vanco)/kg bw/day + 3 mg PFOS/kg bw/day. The experiment was started at PD55, with treatments administered daily by oral gavage for 7 days from PD56 until PD62. Doses were calculated each day based on bodyweight. Treatment concentrations were selected based on a review of available literature. Cages were fitted with aspen wood chip bedding (Tapvei, Denmark). The rats were kept in cages (High Temperature Polysulfonate) placed in ScanTainers (ventilated cabinets, Scanbur) with ScanClime (Scanbur) controlled environmental conditions, with reversed light/dark cycles of 12 h, humidity 55 ± 5%, temperature at 22 ± 1 °C, with air change at 50 times per hour. Feed was given ad libitum with soy and lucerne free feed based on Altromin 1314 (Altromin GmbH, Germany) containing 1.52 mg/kg iodine and 0.26 mg/kg selenium. Acidified tap water was given ad libitum in BPA free bottles (84-ACBT0702SU, Techniplast, PA, USA).

The animal experiments were carried out in the BioFacility of the Technical University of Denmark. Ethical approval was obtained from the Danish Animal Experiments Inspectorate, authorization number 2020-15-0201-00570. The experiments were overseen by the in-house Animal Welfare Committee for animal care and use at the National Food Institute.

2.2. Autopsies/tissue samples

All 48 rats were weighed before being anesthetized with CO_2/O_2 and killed by decapitation. Trunk blood for serum hormone quantification was kept on ice (<1 h) before centrifugation at 4000 rpm at 4 °C for 10 min. Livers and thyroid glands were weighed. Subsequently, hypothalami (including ventromedial nucleus and perifornical TRH neurons, as described by Merchenthaler and Liposits, 1994), pituitaries, thyroids, and livers were collected in RNAlater (Ambion Inc., CT, USA) for bulk-RNA sequencing (n = 12) according to suppliers' protocol and stored at −80 °C. Liver samples (n = 3/group) for histology were excised and fixed in 10% neutral buffered formalin (24 h), before being tissue processed (Excelsior AS Tissue Processor, Thermo Scientific, United Kingdom) and embedded in paraffin.

2.3. Thyroid hormone analysis by LC-MS^2

Serum samples were extracted as previously described (Hansen et al., 2016), with slight modifications. In brief, 50 μL serum was spiked with isotopic-labelled (^{13}C)-thyroid hormone standards (internal standards (IS), cT2, cT3 and cT4) and homogenized. After antioxidant treatment (0.1 mL, 25 mg/mL ascorbic acid, R,R-dithiothreitol and citric acid solution) and protein denaturation by urea (8 M in 1% NH4OH), the samples were enriched using solid-phase micro-extraction (SOLAμ HRP 10 mg/1 mL 96 well plate, Thermo Fisher Scientific, Germany) and reconstituted in 100 μL 5% methanol containing an instrument control standard (ICS, crT3). Procedural blanks containing water instead of plasma were included from the beginning.

The targeted analysis of THs was performed on an Agilent 6495c triple-quadrupole system with a hyphenated Agilent 1290 Infinity II UHPLC system (binary pump, degasser, and autosampler; Agilent Technologies). Targeted analytes were thyroxine (T4), 3,3′,5-triiodothyronine (T3), 3,3′,5′-triiodothyronine (rT3), 3,5-diiodothyronine (3,5-T2), 3,3-diiodothyronine (3,3-T2), 3-iodothyronine (T1), thyronine (T0), 3-iodothyroacetic acid (T1Ac), 3,5-Diiodothyroacetic acid (Diac), triiodothyroacetic acid (Triac) and tetraiodothyroacetic acid (Tetrac). Quantifiable hormones in our samples were T4, T3, rT3, T1Ac and T0. Neat standard ten-point equimolar calibration curves (0.04–20.0 pmol/mL TH, n = 2) were prepared in 5% methanol and all vials contained a fixed amount IS and ICS (15.2 pmol/mL). Data analysis was conducted in MassHunter version 10.1 (Agilent Technologies). Detailed descriptions of chemicals and reagents, the extraction method, instrumental parameters, as well as limits of detection and limits of quantification, are found in supplementary file (S1_Supplemental_Methods).

2.4. TSH analysis

Serum TSH was quantified in technical duplicates (n = 9–10) using MILLIPLEX MAP Rat Pituitary Magnetic Bead Panel(RPTMAG-86 K) from Millipore (MA, USA) (LOQ = 0.87 pg/mL). The kit was used with a Bio-Plex 200 Array Reader from Bio-Rad (CA, USA) according to the manufacturer's protocol. TSH concentration was estimated using a linear trendline (R^2 = 0.9948) based on the supplied standard.

2.5. RNA isolation

Total RNA was isolated using AllPrep DNA/RNA/Protein Kit from Qiagen (Germany) according to manufacturer's instructions and stored at −80 °C. RNA concentrations were determined using a Nanodrop spectrometer (ND-1000, Fisher Scientific), and quality was evaluated using a Bioanalyzer (Agilent Technologies, CA, USA), with acceptable RNA integrity number (RIN) score set to >6. All RNA samples were diluted to 25 ng/μL in a 96-well PCR plate, and stored in −80 °C before library preparation and sequencing.

2.6. Bulk RNA barcoding (BRB) library preparation and sequencing

The 3′ Bulk RNA Barcoding and sequencing (BRB-seq) (Alpern et al., 2019) was performed as previously described (Giacosa et al., 2021). In short, the initial reverse transcription and template switching were done using 10 ng total RNA in 4 μL. cDNA was then purified, and double-stranded (ds) cDNAs were made by PCR. 50 ng of ds cDNA was used to build the sequencing libraries by tagmentation with the Illumina Nextera XT Kit (Illumina, #FC-131-1024) according to the manufacturer's recommendations. The resulting library was sequenced using an Illumina NovaSeq 6000 sequencing system. RTA 2.7.7 and bcl2fastq 2.17.1.14 was used for image analysis and base calling. DimerRemover was used to remove adapter dimer reads (https://sourceforge.net/projects/dimerremover/).

2.7. Preprocessing of BRB-seq raw data

The quality control pipeline for preprocessing is described in detail in (Giacosa et al., 2021). In short, 16 bases are initially read, and all must have a quality score >10. The unique sample-specific barcode corresponds to first 6 bp, and the unique molecular identifier (UMI) corresponds to the following 10 bp. Rat reference transcriptome from the UCSC website (release rn6, downloaded in August 2020) using BWA version 0.7.4.4 with the parameter "–l 24" was used to align the second reads. Read mapping to multiple positions in the genome were removed from the analysis. Following quality control and data preprocessing, UMIs associated with each gene (lines) in each sample (columns) was used to create a gene count matrix. Normalization of the UMI matrix was conducted using regularized log (rlog) transformation package from the DeSeq2 package (Love et al., 2014). Raw and preprocessed data were deposited at the GEO repository under the accession number GSE196133 (Edgar et al., 2002).

2.8. Differential gene expression and functional analysis

Differentially expressed genes (DEGs) were identified using the AMEN suite of tools (Chalmel and Primig, 2008). Statistical comparisons were made independently for each organ (hypothalamus, pituitary, thyroid, and liver): samples exposed to Vancomycin vs controls, samples exposed to PFOS vs Controls, and samples exposed to PFOS and Vancomycin vs controls (Chalmel and Primig, 2008). Briefly, genes showing an expression signal higher than a given background cutoff (corresponding to the overall median of the rlog-transformed UMI dataset, 3.46) and at least a 1.5-fold change relative to the control groups were selected. Statistically significant DEGs were identified by using the empirical Bayes moderated t-statistics implemented into the LIMMA package (F-value adjusted using the Benjamini & Hochberg (BH) False Discovery Rate approach, $p \leq 0.05$) (Ritchie et al., 2015; Smyth, 2004). For each organ, the resulting set of DEGs were then clustered into distinct expression patterns with the k-means algorithm and presented as heatmaps. Gene ontology (GO) enrichment was conducted for each gene cluster using AMEN (Chalmel and Primig, 2008), with an BH-adjusted *p value* of ≤ 0.05. The resulting toxicogenomic signatures were submitted at the TOXsIgN repository under the accession number TSP1265 (https://toxsign.genouest.org) (Darde et al., 2018).

2.9. Statistical analysis

Weight and hormone data were checked for normality using qqplot and Bartlett's test for variance before One-way ANOVA followed by post hoc Tukey test or Kruskal-Wallis with post-hoc Dunn's test. Statistically significant results are presented with (*), $p < 0.05$, as determined by statistical analysis.

The remaining graphs were generated using Graphpad Prism 9 (Graphpad, CA, USA) and Adobe Illustrator 2020 (Adobe, CA, USA).

3. Results

Both PFOS and vancomycin treatment affected liver weight.

Liver weights relative to body weights were significantly increased in the PFOS-treated groups when compared to the controls, whereas vancomycin treatment reduced the relative liver weights compared to controls (Fig. 1A). Absolute liver weights were not significantly different in the PFOS-treated group when compared to controls, whereas they were significantly lower in the vancomycin-treated group relative to the PFOS-treated group (data not shown). Body weight gain at study termination (data not shown) and thyroid gland weights (absolute and relative to body weight) were unaffected across all treatment groups compared to controls (Fig. 1B).

3.1. PFOS lowered serum TH, but not TSH levels

After 7 days of exposure to PFOS, total serum concentration of T4, T3, rT3 and T1Ac were significantly reduced compared to control animals, whereas no effects were observed for T0 (Fig. 2A–E). Vancomycin did not affect TH concentrations, nor did vancomycin change the effects of PFOS during co-treatment: the effects of PFOS only and with and without vancomycin were similar. The change in circulating thyroid hormones were not accompanied by a significant change in TSH (Fig. 2F).

3.2. PFOS induced lipid accumulation in the liver

Livers were stained with H&E for histology examination, as detailed in supplementary file "S1_Supplemental_Methods". Livers were examined for lipid droplet formation in zone 1, 2, and 3 of the lobules. The PFOS-exposed groups showed signs of lipid droplet accumulation when compared to controls (Figure S1, S2_Supplementary_Figures). Only modest signs of lipid accumulation were observed in the control, vancomycin, and vancomycin + PFOS treated groups.

3.3. Transcriptomics revealed organ-specific effects of PFOS exposure

The transcriptomic analysis identified 50 DEGs in the hypothalamus, 68 in the pituitary, 71 in the thyroid gland, and 181 in the liver (Fig. 3A–D, S3_Table_RNA-seq_DEGs) which further clustered into 3, 3, 4, and 7 expression patterns in the distinct organs, respectively. Most of the genes were affected by PFOS exposure rather than by vancomycin treatment. A functional analysis was performed to determine whether some of those expression patterns are significantly associated with specific biological processes and pathways (S4_Table_Functional_analysis).

In the hypothalamus, the 50 DEGs were partitioned into three broad expression patterns denoted Hy1-3 to accurately represent the trends in the data (Fig. 4A). Pattern Hy1 was generally upregulated in response to PFOS exposure. The general expression trend for pattern Hy2 was downregulation following PFOS exposure, whereas vancomycin did not seem to affect expression notably. For pattern Hy3, there was a general downregulation induced by both vancomycin and PFOS exposure, with a combination of the two groups resulting in an even stronger downregulation. Of these, only pattern Hy2 was significantly associated with GO terms, of which there were 26 (Figure S3A,

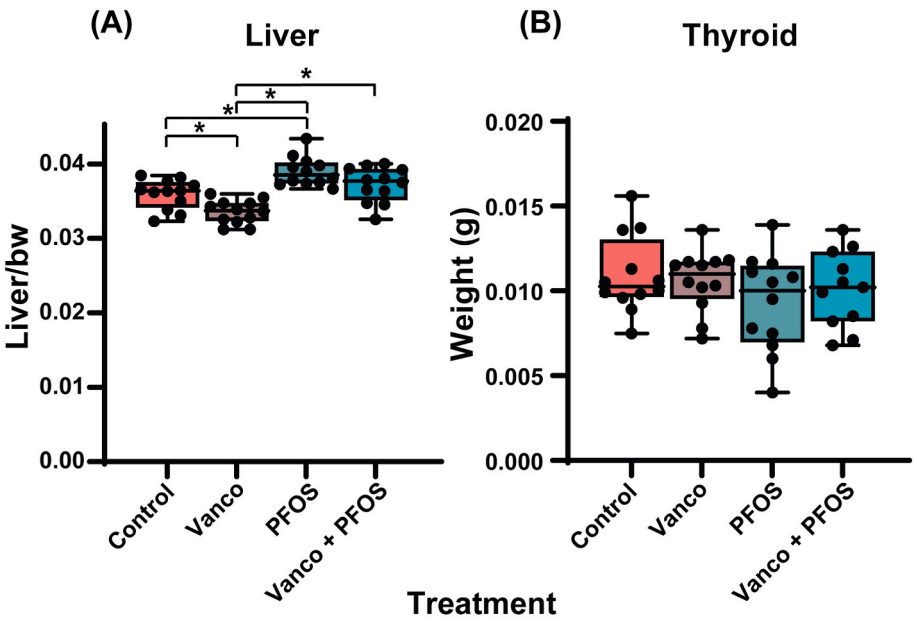

Fig. 1. Exposure to PFOS and vancomycin alters liver weights, but not thyroid weights, in adult male rats. Male rats were treated with either vehicle control (red), 8 mg/kg/day vancomycin (vanco) (brown), 3 mg/kg/PFOS (blue), or 8 mg/kg/day vancomycin + 3 mg/kg/day PFOS (turquoise) for 7 days. Weights are presented as box plot with (•) denoting individual measurements (n = 12), in addition to mean, 25th to 75th percentile, and whiskers showing minimum and maximum values. Statistically significant results are presented with (*), $p < 0.05$, as determined by one-way ANOVA with post-hoc Tukey's test (For interpretation of the references to color in this figure legend, the reader is referred to the Web version of this article.)

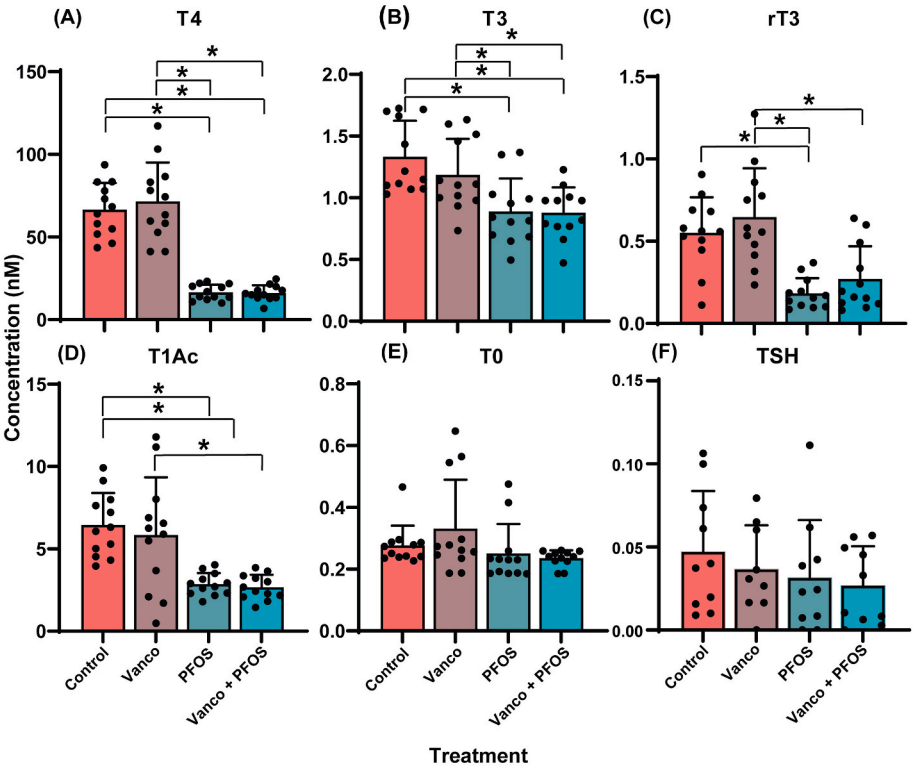

Fig. 2. Circulating thyroid hormone levels decreases in response to PFOS exposure: (A) T4, **(B)** T3, **(C)** rT3, and **(D)** T1Ac decreased with PFOS exposure, **(E)** T0 and **(F)** TSH were unaffected. Blood samples were collected at experiment termination following 7 days exposure to either vehicle control (red), 8 mg/kg/day vancomycin (vanco) (brown), 3 mg/kg/day PFOS (blue), or 8 mg/kg/day vancomycin + 3 mg/kg/day PFOS (turquoise). Data is shown as mean ± SD with each (•) representing each data point. Hormones were measured by either LC-MS^2 (n = 12) **(A–E)** or Milliplex kit (n = 9–10) **(F)**. Statistically significant results are presented with (*), $p < 0.05$, as determined by one-way ANOVA (B, F) with post-hoc Tukey's test or Kruskal-Wallis (A, C-E) with post-hoc Dunn's test. (For interpretation of the references to color in this figure legend, the reader is referred to the Web version of this article.)

S2_Supplementary_Figures). The GO-terms with the highest representation were axon (GO:0030424, 12 genes, *p value* < $4.0e^{-7}$) and neuron projection (GO:0043005, 13, $3.2e^{-5}$), plasma membrane bounded cell projection (GO:0120025, 13, $1.5e^{-3}$), and cell projection (GO:0042995, 13, $1.6e^{-3}$). This suggests dysregulation of genes related to neuronal communication in the hypothalamus.

For the pituitary, the 68 DEGs were clustered into three expression patterns denoted Pi1-3 (Fig. 4B). In pattern Pi1, there was a general upregulation with all treatment groups. In pattern Pi2, all groups showed a general upregulation, except the vancomycin treated group, which was downregulated. For pattern Pi3 there was a general downregulation in all groups. However, no functional terms were significantly associated within these. To our knowledge, neither of the functional terms associated with the TH system. This was further evident by the fact that none of the 68 DEGs are key factors of the HPT axis.

In the thyroid, 71 DEGs were partitioned into four expression patterns denoted Ty1-4 (Fig. 4C). Pattern Ty1 was generally upregulated by PFOS treatment, but these effects seem to be counteracted by the presence of vancomycin. PFOS treatment caused a general upregulation in pattern Ty2, which again seemed to be slightly counteracted by the presence of vancomycin. Pattern Ty3 was generally downregulated by the presence of PFOS, and in pattern Ty4, there was a general

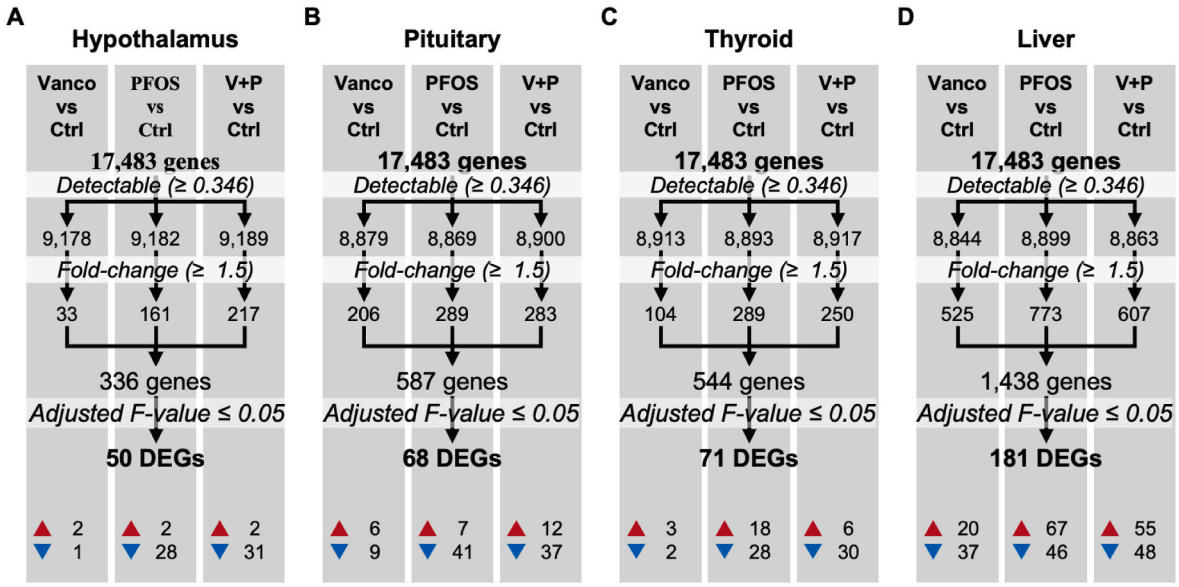

Fig. 3. RNA-sequencing revealed that the liver had the most differentially expressed genes (DEGs). RNA collected from hypothalamus, pituitary, thyroid, and liver was sequenced with BRB-seq. RNA was collected from organ samples collected following 7 days exposure to either corn oil (control, ctrl), 8 mg/kg/day vancomycin (vanco, v), 3 mg/kg/day PFOS (p), or 8 mg/kg/day vancomycin and 3 mg/kg/day PFOS. DEGs were identified by comparing treatment groups to the control group using limma. Threshold for DEGs was set to ≥1.5 fold-change and significance was determined using adjusted F-value ≤ 0.05. The final number of DEGs per group correspond to unique genes within each organ, with the discrepancy in total number of individual up- or down-regulated DEGs corresponding to genes shared between two or more groups (i.e. for hypothalamus the 50 DEGs represents 50 unique genes amongst the 66 DEGs observed between the three exposure groups).

downregulation with all treatments. Among those four expression patterns, only patterns Ty1 and Ty3 were significantly associated with enriched functional terms. Pattern Ty1, with the GSEA term «PHONG_TNF_RESPONSE_NOT_VIA_P38», had 7 DEGs: *Jund*, *Larp6*, *Sox9*, *Tmem265*, *Wtap*, *Optn*, and *Plcb1* (7, $9.8e^{-3}$). Pattern Ty3, with the GSEA term «SENESE_HDAC1_TARGETS_DN», had 5 DEGs: *Baz2B*, *Cdc42ep3*, *Igfbp5*, *Sesn3*, and *Utrn* (5, $5.8e^{-3}$). None of the 71 DEGs identified in the thyroid are, to our knowledge, regulated by TSHr or implicated in TH synthesis or the TH system in general.

In the liver, the 181 DEGs were partitioned into seven expression patterns denoted Li1-7 (Fig. 4D). Pattern Li1 showed general upregulation in all treatment groups. The expression trend in pattern Li2 suggests a general upregulation by PFOS that is counteracted by the presence of vancomycin. Pattern Li3 showed upregulation in both groups treated with PFOS. Pattern Li4 showed an increasing upregulation in response to both vancomycin and PFOS, as well as the combination of the two. For pattern Li5, there was a downregulation with vancomycin treatment that was counteracted by PFOS. Pattern Li6 showed slight upregulation following vancomycin treatment that was counteracted by PFOS. In pattern Li7, there was a general downregulation in all treatment groups. Of these, only two patterns had identifiable functional terms that were significant (Figure S3B, C). Pattern Li2 was associated with a total of 18 GO terms, including cytosol (GO:0005829, 11, $1.9e^{-2}$), translation (GO:0006412, 7, $1.5e^{-2}$), amide biosynthethic process (GO:0043604, 7, 0.032), peptide metabolic process (GO:0006518, 7, $3.3e^{-2}$), and peptide biosynthethic process (GO:0043043, 7, $1.5e^{-2}$). Pattern Li3 showed 56 GO terms, including lipid metabolic process (GO:0006629, 18, $1.81e^{-9}$), small molecule metabolic process (GO:0044281, 18, $1.04e^{-7}$), carboxylic acid metabolic process (GO:0019752, 17, $2.53e^{-10}$), oxoacid metabolic process (GO:0043436, 17, $4.0e^{-10}$), and organic acid metabolic process (GO:0006082, 17, $4.26e^{-10}$). This suggests disruption to several pathways in the exposed livers, particularly those related to lipid and fatty acid metabolism, and xenobiotic response elements.

A comparison of DEGs between the four organs revealed that DEGs were foremost specific to each organ. However, there were also overlapping DEGs in the different patterns of the four organs, albeit very few (Fig. 4E). For example, the neuronal guidance factor *Sema3a* was downregulated in both hypothalamus and pituitary of PFOS-exposed rats, whereas the actin-regulatory protein *Tmod2* was downregulated in hypothalamus but upregulated in pituitary. There were DEGs shared between pituitary and liver, such as *Coa5*, *Mtmr1, Vcl* and *Tob1* that were all downregulated, but are genes that do not immediately point towards any shared functional term. Other examples include the CYP family member *Cyp2u1,* which was downregulated in pituitary but upregulated in thyroid of PFOS-exposed rats. Genes that were downregulated in liver, but upregulated in thyroid, such as *Crebbp* and *Jund*, and several genes that were downregulated in both hypothalamus and thyroid, including *Slc38a1*, *Sptbn1*, *Trmtc4* and *Plcb1*. Again, these factors may point to important functions individually, but do not immediately enrich specific functional terms.

PFASs are known to affect Wnt signaling (Yang et al., 2020), so we used the Kyoto Encyclopedia of Genes and Genomes (KEGG) pathway resource implemented into the pathview tool (Luo and Brouwer, 2013) to display potential DEGs relevant to Wnt signaling. Irrespective of GO functional terms, it revealed that some genes of the Wnt signaling pathway were affected by PFOS exposure when combining DEGs from all organs, for instance the G protein-coupled receptor *Frizzled* (Fig. 5). Similarly, some of the DEGs identified in the animals exposed to PFOS are known to be involved in MAPK, calcium, or PPAR signaling pathways (Figure S4-S6, S2_Supplementary_Figures). Notably, none of the identified DEGs aligned with thyroid hormone signaling pathway.

4. Discussion

PFOS can disrupt the TH system in animals and humans. In rats, typical effects of exposure are reduced T4 and T3 levels in the serum without a compensatory increase in TSH. Herein, we induced this hypothyroxinemia-like effect-pattern at a non-toxic concentration and subsequently analysed the transcriptomes of several organs of the TH system. The exposure design proved to be fit-for-purpose in that exposed animals displayed no significant changes in body weight and only slight increase in liver weights without any overt signs of histopathological

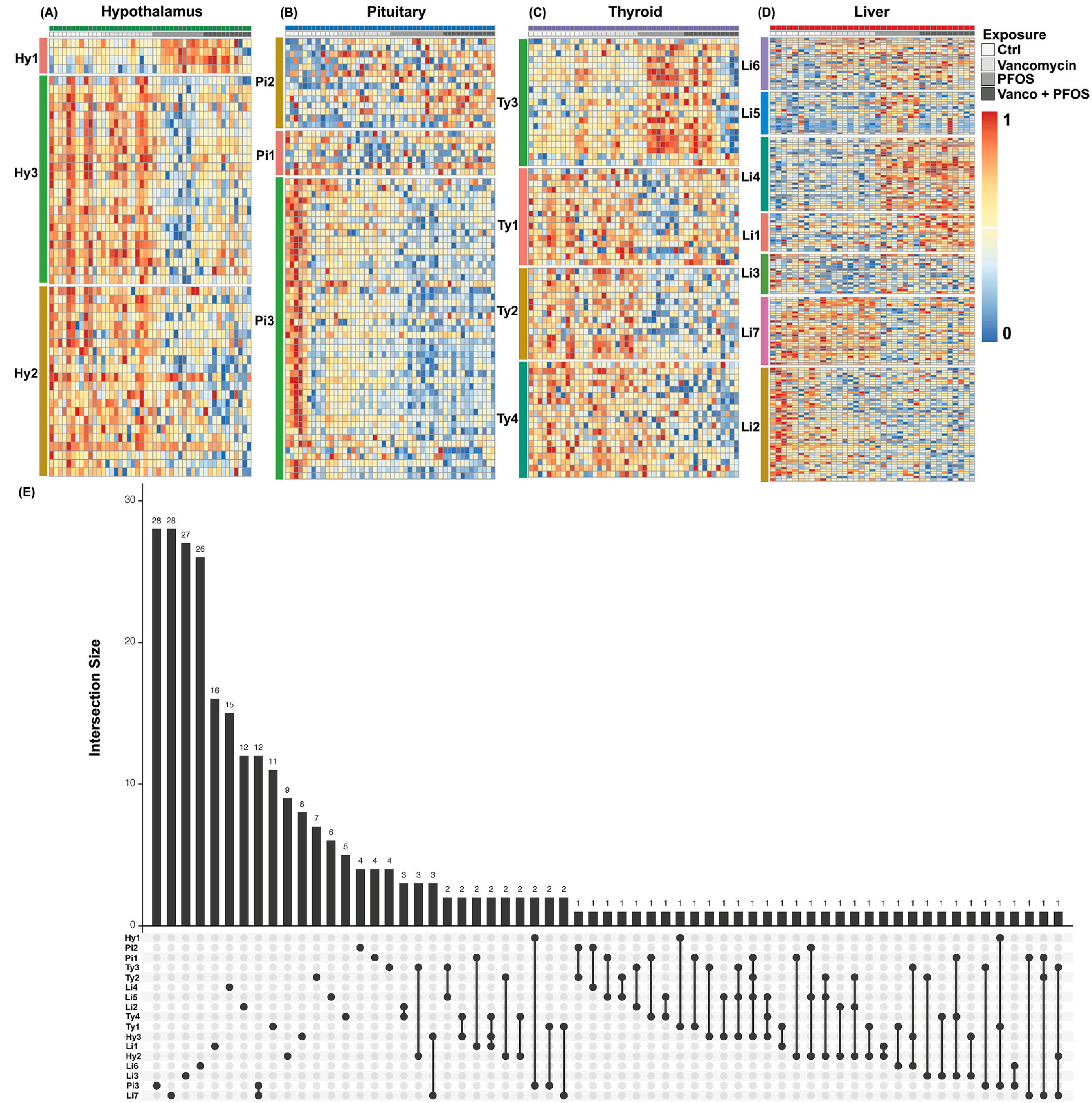

Fig. 4. Clustering analysis shown as heatmaps, the hypothalamus and liver had most GO terms. RNA collected following 7 days of exposure to either control (ctrl), 8 mg/kg/day vancomycin (vanco), 3 mg/kg/day PFOS, or 8 mg/kg/day vancomycin +3 mg/kg/day PFOS was sequenced using BRB-seq. Results from the tissues hypothalamus (Hy)**(A)**, pituitary (Pi) **(B)**, thyroid (Ty) **(C)**, and liver (Li) **(D)** were clustered into patterns after filtering and testing for significance. Shared differentially expressed genes (DEGs) between the different patterns are shown in the intersection plot **(E)**.

changes. Further, serum TH levels were significantly reduced in the animals exposed to PFOS for 7 days, recapitulating effects seen for both T3 and T4 in previous animal studies (Chang et al., 2008; Coperchini et al., 2017; Schrenk et al., 2020; Seacat et al., 2002; Thibodeaux et al., 2003; Yu et al., 2009). We also found that the TH metabolites rT3 and T1Ac were reduced, which indicates that the PFOS effect profile extends beyond T3 and T4. Finally, we saw no changes to TSH levels in serum, nor changes to thyroid gland weights, supporting the fact that TSH is not elevated in response to the pronounced drop in serum T4 and T3.

An additional aim of our study was to see if an altered microbiota would alter the effects of PFOS exposure and, in turn, induce different effects on the TH system. For this, we chose to treat one PFOS-exposure group with vancomycin, as it reportedly does not cross the gut epithelium (Rao et al., 2011). Although vancomycin treatment resulted in reduced liver weights, we observed no obvious difference in the transcriptome in response to PFOS exposure in the vancomycin-treated animals when comparing to animals exposed to only PFOS. This suggests that, in the given context, the microbiota did not play a significant role in PFOS-induced effects on TH levels.

Having established that PFOS exposure induced the expected

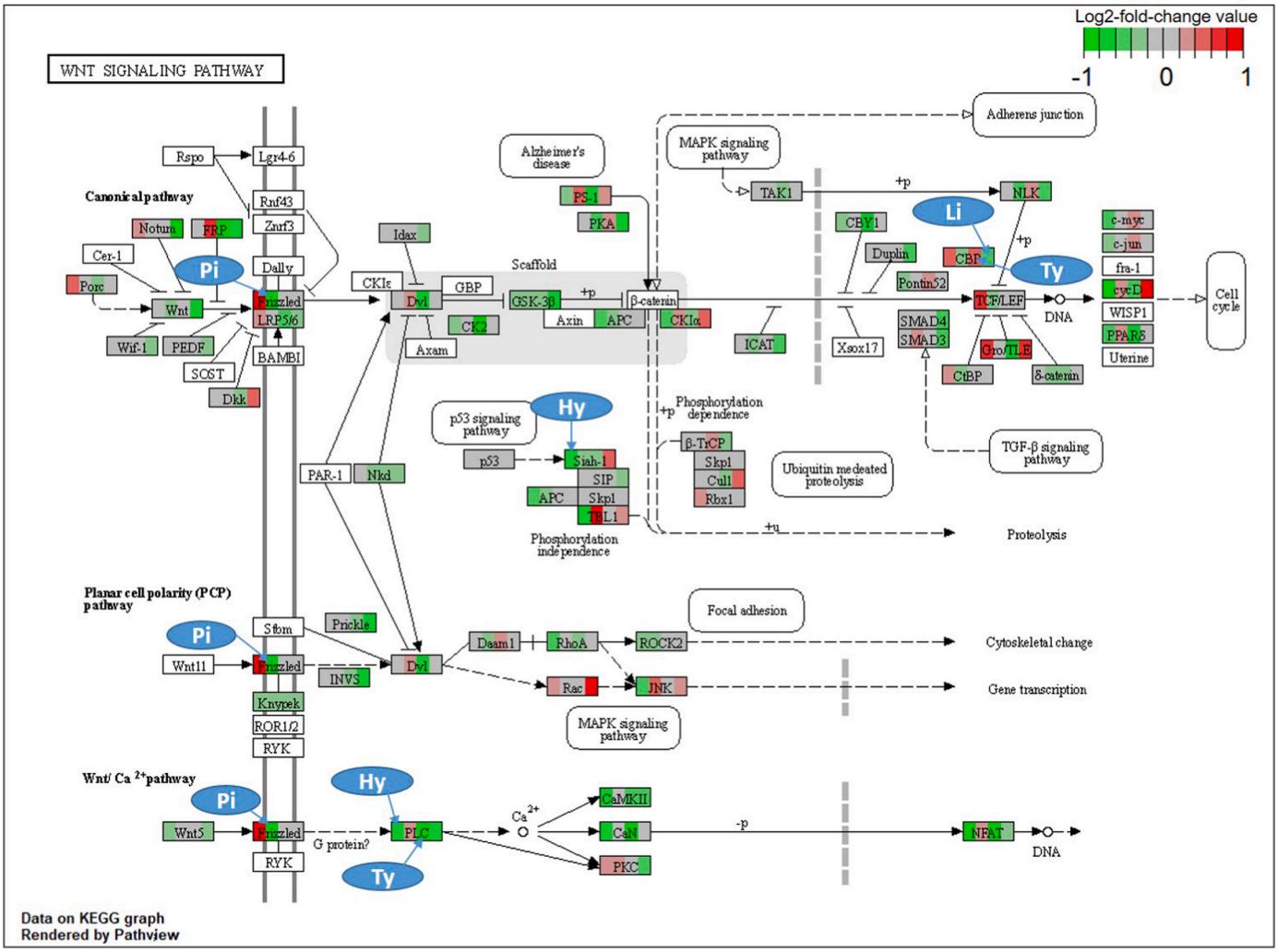

Fig. 5. Genes of the WNT signaling pathway affected by PFOS exposure in different organs. When compared to controls, adult rats exposed to PFOS display some dysregulated genes in different organs. Each gene is represented in a box with four sub-boxes color-coded (green = downregulated; red = upregulated) according to its log2-fold change expression (PFOS vs Ctrl) in the order, left to right: hypothalamus (Hy), pituitary (Pi), thyroid (Ty) and liver (Li). In the pituitary, *Frizzled (Fzd1)* was significantly downregulated. Both *siah E3 ubiquitin protein ligase 1 (Siah1)* and *phospholipase C β 1 (Plc)* were downregulated in the hypothalamus (Hy). In the thyroid (Ty), *Plc* was also downregulated, whereas *CREB binding protein (Cbp)* was upregulated. Finally, in the liver (Li), *Cbp* was downregulated. (For interpretation of the references to color in this figure legend, the reader is referred to the Web version of this article.)

hypothyroxinemia-like effects on the TH system, the main aim of the study was addressed; namely, characterizing changes to the transcriptome of central tissues of the HPT-axis and TH system. Hypothalami, pituitaries, thyroids, and livers were subjected to bulk-RNA sequencing to determine the effects of PFOS in each tissue, and whether the tissues had responded to reduced circulatory concentrations of T3 and T4. This was done to improve our understanding of the systemic effects of PFOS and, hopefully, begin to unravel effects of PFOS exposure on the TH system or on organs of the TH system regulation axis, being it direct effects of PFOS exposure or indirectly by occurring downstream of TH system disruption. As expected, the liver was the most affected organ at the transcriptional level in response to PFOS exposure, but the hypothalamus, pituitary and thyroid all displayed some transcriptional changes. We also observed minor differences in DEGs from animals exposed to PFOS only versus vancomycin-treated animals exposed to PFOS. However, the differences between these groups were minor, suggesting that the altered gut microbiota had little impact on the observed effects on the TH system.

Although 71 DEGs were identified in the thyroids of exposed animals, none of these genes are known to play a role in TH synthesis. Only a few interesting DEGs were identified, such as increased expression of *Sox9*, *Jund*, and *Larp6*. The function of SOX9 in the thyroid gland during adulthood is not well understood, but knockdown of *Sox9* inhibits proliferation and invasion of human thyroid cancer cells (Huang and Guo, 2017). Both *Sox9* and *Jund* have been associated with benign thyroid tumors in humans (Wang et al., 2018), lending some support to the suggestion that PFOS exposure may be involved in thyroid cancer development (Butenhoff et al., 2012). The general findings in the thyroid glands suggest two primary results. Firstly, PFOS does not directly target TH synthesis at the gene transcription level and hence, the TH synthesis apparatus is intact. Therefore, it seems unlikely that PFOS reduce serum TH through a thyroid gland mediated mechanism (Chang et al., 2008; Ramhøj et al., 2020). Secondly, the untargeted gene expression analysis revealed that transcript levels of the TSH and TSH receptor-regulated genes were unaffected. This strongly suggests that the thyroid gland in PFOS-exposed animals were not stimulated by increased TSH action, which is supported by unaffected TSH levels and thyroid gland weight. These findings also support, and extend on, previous targeted investigations of PFOS and other PFASs conducted in rats (Chang et al., 2008; Gilbert et al., 2021; Ramhøj et al., 2020, 2018; W.-G. Yu et al., 2009). Notably, while our results rule out effects at the transcript level, we cannot rule out possible effects at the protein level;

either expression or function.

We observed 68 DEGs in the pituitaries of animals exposed to PFOS only, none of which are, to our knowledge, key factors involved in TSH regulation or synthesis. This suggests that, at the transcript level, reduction in THs induced by PFOS fails to activate a response in the pituitary including the *Tshb*-gene encoding the TSHβ-subunit of TSH. Our data cannot answer whether lack of TSH induction directly stems from reduced TRH stimulation of the pituitary. However, a reduction in TRH stimulation would presumably result in decreased expression of genes such as *Tshb* (Steinfelder et al., 1991), which we did not observe. Looking further at the pituitary, we observed no changes in serum TSH levels, which corroborates previous studies (Chang et al., 2008; Coperchini et al., 2017; Schrenk et al., 2020; Seacat et al., 2002; Thibodeaux et al., 2003; W. G. Yu et al., 2009).

In the hypothalamus, we observed 50 DEGs in the PFOS exposure group, which was the smallest transcriptional effect among the analysed tissues. Unlike the pituitary and thyroid, however, multiple GO-terms were identified. Many of the GO-terms and related genes are involved in brain neuronal function, but a few genes may also suggest that PFOS could affect hypothalamic TRH secretion through neurons in the paraventricular nuclei (PVN). PFOS exposure downregulated *Myo5a*, an actin-dependent transport motor which moves neuropeptides and hormones along axons and dendrites in large dense core vesicles (LDCVs) (de Wit et al., 2006; Rudolf et al., 2011). There are indications that TRH is released from LDCVs, and LDCV release is thought to be affected by glutamatergic signaling (Hrabovszky et al., 2005; Yin et al., 2015). Notably, *Sema3a* was also downregulated by PFOS exposure. SEMA3A is, like TRH, transported through LDCVs (Hrabovszky et al., 2005; Rudolf et al., 2011; Yin et al., 2015) and functions as an axon guiding protein (Yoshida, 2012) involved in neuronal plasticity, recovery from injury in the nervous system and dendritic spine density in the adult brain (Morita et al., 2006; Pasterkamp and Giger, 2009; Yoshida, 2012). In addition to effects mediated through glutamate signaling, PFOS may also inhibit prolactin secretion by affecting GABAergic cells in the paraventricular nuclei (PVN) (Salgado et al., 2015). Prolactin, like TSH, is secreted from the pituitary and regulated by the PVN of the hypothalamus in rats (Salgado et al., 2016, 2015). This suggests that PFOS exposure affects the hypothalamus in a way that could impact TRH regulation. However, the HPT axis is still functional in PFOS-exposed male rats (Chang et al., 2008). Nevertheless, our results suggest that PFOS could affect TRH regulation directly, albeit our study design precludes the possibility to address this specifically.

We also found the GABA-related genes *Rab2a, Slc38a1, Gad2*, and *Gabra2* (Betley et al., 2009) to be downregulated by PFOS treatment. The specific function of *Rab2a* in the brain is not well understood, but has been associated with reduced prefrontal cortical thickness and density of calbindin-immunoreactive interneurons, a type of GABAergic neurons involved in working memory (Kim and Webster, 2010; Li et al., 2015). Another gene that was significantly downregulated in both of the PFOS treated groups was *Plcb1*, a gene associated with a number of neurological disorders in humans (Yang et al., 2016). *Plcb1* was also affected in both the pituitary and thyroid, suggesting a common and direct effect of PFOS exposure. Numerous other studies have found effects of PFAS exposure on the nervous system (Wang et al., 2019). For instance, in a study with PFOS exposure of 3 mg/kg, PFOS altered dopamine levels and the dopamine receptor (Salgado et al., 2016). Several mechanisms for PFOS-mediated effects on brain function have been suggested (Wang et al., 2019). Importantly, however, it is still difficult to discriminate between effects that may be caused directly by PFOS exposure and those that potentially are caused by a lack of TH in the hypothalamus or the brain. Further studies are needed to understand the extent of effects on neuronal function in the hypothalamus, as well as effects on TRH release.

The largest transcriptional changes were observed in the livers of exposed animals. A large number of these may be attributed to the capacity of PFOS to activate the nuclear receptors Peroxisome proliferator-activated receptor alpha (PPARα), Constitutive androstane receptor (CAR), or Pregnane X receptor (PXR), as previously reported (Dong et al., 2016; Rosen et al., 2010). In the liver of adult male rats exposed for 28 days to 50 mg PFOS/kg, 593 DEGs were observed (Dong et al., 2016). This is significantly more than the 113 DEGs observed in our study. However, the difference may be attributed to the higher exposure dose and longer exposure duration used by Dong et al. (2016). Both studies suggest that the liver is strongly affected by PFOS.

It is well established that PFASs can activate PPARα (Rosenmai et al., 2018; Takacs and Abbott, 2007; Wolf et al., 2008), as well as CAR and PXR (Dong et al., 2016; Elcombe et al., 2012; Rosen et al., 2008), leading to upregulation of phase I and phase II enzymes. PFOS exposure has also been shown to increase excretion of TH through bile and urine in rats (Chang et al., 2008), which indicates activation of hepatic enzymes and ultimately excretion of TH. Signaling pathways such as PPARα, CAR, and PXR are possible mediators of such activation, leading to upregulating glucuronidating and sulfonating enzymes. However, the specific enzymes identified in this study are not known to target TH.

Liver enzyme induction is not the only mechanism that can lead to increased TH excretion. Displacement of TH by chemical binding to TTR can also lead to increased liver TH metabolism and excretion. Although our study was not specifically designed to identify these mechanisms, it is known that PFOS can bind to TTR and rapidly displace T4 to the circulation (Ren et al., 2016; Weiss et al., 2009). Based on our results, and other reports on PFOS and liver enzyme induction (Dong et al., 2016; Rosen et al., 2017; W.-G. Yu et al., 2009), as well as TTR binding, it is possible that increased TH excretion plays a role in serum TH reductions associated with PFOS exposure, but the evidence is not overwhelmingly convincing. Interestingly, liver enzyme induction and TTR-binding are mechanisms shared between many environmental chemicals that reduce serum T4 without increasing TSH (Bansal et al., 2014; Farmer et al., 2018; Goldey et al., 1995; Hamers et al., 2006; Klaassen and Hood, 2001; Kodavanti et al., 2010; Liu et al., 1995; Louis et al., 2017). Future comparative studies should explore how different types of compounds cause different types of thyroid hormone disruption and focus on identifying specific mediators of TH excretion.

Although our thyroid hormone system-disrupted rats did not reveal obvious enrichments or DEGs that are known to be central players in thyroid signaling, KEGG analysis did reveal potential disruptions to other important regulatory pathways. For instance, Wnt signaling, which is affected by PFOS *in vitro* (Yang et al., 2020), showed some signs of disruption in all of the four organs. In addition, DEGs did associate with calcium, MAPK and PPAR signaling pathways. Importantly, multiple genes of the PPAR signaling pathway were dysregulated in the liver, showing that PPAR is a likely target for PFOS. It should be noted, however, that this study has analysed transcriptional changes in the adult rat. In adult animals, the impact of dysregulation to key regulatory pathways may not be as consequential as they would be if exposure occurs during development, for example with Wnt signaling that is crucial for guiding numerous developmental processes. A second point is that these transcriptional changes are just as likely not a consequence of reduced TH levels, but a direct effect of PFOS on target tissues. Our study design cannot distinguish between what effects are caused directly by PFOS or secondary to TH system disruption, or a mixture of the two.

5. Conclusion

We induced a hypothyroxinemia-like effect in male rats by exposing them to PFOS for 7 days. Several DEGs were identified in the liver and organs of the HPT-axis. However, in the pituitaries and thyroid glands none of the identified DEGs are known to be related to TH regulation. Therefore, PFOS does not seem to affect the TH system directly through effects on the thyroid or the pituitary, suggesting that the HPT-axis was not activated to compensate for the reduced TH concentrations. In contrast, our findings lend some support to the general view that upregulation of hepatic enzymes and increased TH excretion may

contribute to PFOS-induced reduction in serum TH, albeit our data does not prove this notion. We also included a PFOS exposure group with compromised gut microbiota in order to test the hypothesis that the gut microbiome can play a role in how individuals respond to environmental exposure. In this study, we did not find any obvious effects on the transcriptional level in the analysed organs; yet, we would still suggest that including this parameter in future studies would be important.

Author statements

Nichlas Davidsen: Conceptualization, Data curation, Formal analysis, Investigation, Visualization, Writing – original draft, Writing – review & editing. Louise Ramhøj: Conceptualization, Data curation, Formal analysis, Investigation, Supervision, Writing- original draft, Writing – review & editing. Claus Asger Lykkebo: Conceptualization, Formal analysis, Investigation, Writing – review & editing. Indusha Kugathas: Formal analysis, Writing – review & editing. Rikke Poulsen: Data curation, Writing – review & editing. Anna Kjerstine Rosenmai: Formal analysis, Writing – review & editing. Bertrand Evrard: Data Curation, Writing – review & editing. Thomas A. Darde: Data curation, Writing – review & editing. Marta Axelstad: Formal analysis, Writing – review & editing. Martin Iain Bahl: Methodology, Writing – review & editing. Martin Hansen: Methodology, Writing – review & editing. Frederic Chalmel: Data curation, Formal analysis, Visualization, Methodology, Writing – review & editing. Tine Rask Licht: Funding acquisition, Supervision, Writing – review & editing. Terje Svingen: Conceptualization, Funding acquisition, Project Administration, Supervision, Writing – original draft, Writing – review & editing.

Funding

This study received funding from The Danish Veterinary and Food Administration. The funding body had no role in study design, data interpretation or decision to publish. MH acknowledge the financial support from Aarhus University Research Foundation (AUFF-T-2017-FLS-7-4) and the European Union's Horizon 2020 research and innovation program, under grant agreement No. 825753 (ERGO).

Declaration of competing interest

The authors declare that they have no known competing financial interests or personal relationships that could have appeared to influence the work reported in this paper.

Acknowledgements

We want to thank our technicians, Lillian Sztuk, Dorte Lykkegaard Korsbech, Mette Voigt Jessen, Heidi Letting and Katja Ann Kristensen, for their invaluable contributions. Histology data was generated though accessing research infrastructure at DTU National Food Institute, including FOODHAY (Food and Health Open Innovation Laboratory, Danish Roadmap for Research Infrastructure).

Appendix A. Supplementary data

Supplementary data to this article can be found online at https://doi.org/10.1016/j.envpol.2022.119340.

References

Alpern, D., Gardeux, V., Russeil, J., Mangeat, B., Meireles-Filho, A.C.A., Breysse, R., Hacker, D., Deplancke, B., 2019. BRB-seq: ultra-affordable high-throughput transcriptomics enabled by bulk RNA barcoding and sequencing, 2019 201 Genome Biol. 20, 1–15. https://doi.org/10.1186/S13059-019-1671-X.

Bansal, R., Tighe, D., Danai, A., Rawn, D.F.K., Gaertner, D.W., Arnold, D.L., Gilbert, M.E., Zoeller, R.T., 2014. Polybrominated diphenyl ether (DE-71) interferes with thyroid hormone action independent of effects on circulating levels of thyroid hormone in male rats. Endocrinol. (United States) 155, 4104–4112. https://doi.org/10.1210/EN.2014-1154/SUPPL_FILE/EN-14-1154.PDF.

Betley, J.N., Wright, C.V.E., Kawaguchi, Y., Erdélyi, F., Szabó, G., Jessell, T.M., Kaltschmidt, J.A., 2009. Stringent specificity in the construction of a GABAergic presynaptic inhibitory circuit. Cell 139, 161. https://doi.org/10.1016/J.CELL.2009.08.027.

Butenhoff, J.L., Chang, S.C., Olsen, G.W., Thomford, P.J., 2012. Chronic dietary toxicity and carcinogenicity study with potassium perfluorooctanesulfonate in Sprague Dawley rats. Toxicology 293, 1–15. https://doi.org/10.1016/J.TOX.2012.01.003.

Chalmel, F., Primig, M., 2008. The Annotation, Mapping, Expression and Network (AMEN) suite of tools for molecular systems biology. BMC Bioinf. 9 https://doi.org/10.1186/1471-2105-9-86.

Chang, S.C., Thibodeaux, J.R., Eastvold, M.L., Ehresman, D.J., Bjork, J.A., Froehlich, J.W., Lau, C., Singh, R.J., Wallace, K.B., Butenhoff, J.L., 2008. Thyroid hormone status and pituitary function in adult rats given oral doses of perfluorooctanesulfonate (PFOS). Toxicology 243, 330–339. https://doi.org/10.1016/J.TOX.2007.10.014.

Coperchini, F., Awwad, O., Rotondi, M., Santini, F., Imbriani, M., Chiovato, L., 2017. Thyroid disruption by perfluorooctane sulfonate (PFOS) and perfluorooctanoate (PFOA). J. Endocrinol. Invest. https://doi.org/10.1007/s40618-016-0572-z.

Coperchini, F., Croce, L., Ricci, G., Magri, F., Rotondi, M., Imbriani, M., Chiovato, L., 2021. Thyroid disrupting effects of old and new generation PFAS. Front. Endocrinol. https://doi.org/10.3389/fendo.2020.612320.

Darde, T.A., Gaudriault, P., Beranger, R., Lancien, C., Caillarec-Joly, A., Sallou, O., Bonvallot, N., Chevrier, C., Mazaud-Guittot, S., Jégou, B., Collin, O., Becker, E., Rolland, A.D., Chalmel, F., 2018. TOXsIgN: a cross-species repository for toxicogenomic signatures. Bioinformatics 34, 2116–2122. https://doi.org/10.1093/BIOINFORMATICS/BTY040.

de Herder, W.W., Hazenberg, M.P., Pennock-Schröder, A.M., Oosterlaken, A.C., Rutgers, M., Visser, T.J., 1989. On the enterohepatic cycle of triiodothyronine in rats; importance of the intestinal microflora. Life Sci. 45, 849–856. https://doi.org/10.1016/0024-3205(89)90179-3.

de Wit, J., Toonen, R.F., Verhaagen, J., Verhage, M., 2006. Vesicular trafficking of semaphorin 3A is activity-dependent and differs between axons and dendrites. Traffic 7, 1060–1077. https://doi.org/10.1111/J.1600-0854.2006.00442.X.

Dong, H., Curran, I., Williams, A., Bondy, G., Yauk, C.L., Wade, M.G., 2016. Hepatic miRNA profiles and thyroid hormone homeostasis in rats exposed to dietary potassium perfluorooctanesulfonate (PFOS). Environ. Toxicol. Pharmacol. 41, 201–210. https://doi.org/10.1016/j.etap.2015.12.009.

Edgar, R., Domrachev, M., Lash, A.E., 2002. Gene Expression Omnibus: NCBI gene expression and hybridization array data repository. Nucleic Acids Res. 30, 207–210. https://doi.org/10.1093/NAR/30.1.207.

Elcombe, C.R., Elcombe, B.M., Foster, J.R., Chang, S.C., Ehresman, D.J., Butenhoff, J.L., 2012. Hepatocellular hypertrophy and cell proliferation in Sprague–Dawley rats from dietary exposure to potassium perfluorooctanesulfonate results from increased expression of xenosensor nuclear receptors PPARα and CAR/PXR. Toxicology 293, 16–29. https://doi.org/10.1016/J.TOX.2011.12.014.

Farmer, W.T., Louis, G.W., Buckalew, A.R., Hallinger, D.R., Stoker, T.E., 2018. Evaluation of triclosan in the Hershberger and H295R steroidogenesis assays. Toxicol. Lett. 291, 194–199. https://doi.org/10.1016/J.TOXLET.2018.03.001.

Fenton, S.E., Ducatman, A., Boobis, A., DeWitt, J.C., Lau, C., Ng, C., Smith, J.S., Roberts, S.M., 2021. Per- and polyfluoroalkyl substance toxicity and human health review: current state of knowledge and strategies for informing future research. Environ. Toxicol. Chem. 40, 606. https://doi.org/10.1002/ETC.4890.

Fröhlich, E., Wahl, R., 2019. Microbiota and thyroid interaction in health and disease. Trends Endocrinol. Metabol. 30, 479–490. https://doi.org/10.1016/J.TEM.2019.05.008.

Giacosa, S., Pillet, C., Séraudie, I., Guyon, L., Wallez, Y., Roelants, C., Battail, C., Evrard, B., Chalmel, F., Barette, C., Soleilhac, E., Fauvarque, M.O., Franquet, Q., Sarrazin, C., Peilleron, N., Fiard, G., Long, J.A., Descotes, J.L., Cochet, C., Filhol, O., 2021. Cooperative blockade of CK2 and ATM kinases drives apoptosis in VHL-deficient renal carcinoma cells through ROS overproduction, 576 13, 576 Cancers 13. https://doi.org/10.3390/CANCERS13030576.

Gilbert, M.E., O'Shaughnessy, K.L., Axelstad, M., 2020. Regulation of thyroid disrupting chemicals to protect the developing brain. Endocrinology 161 (10). https://doi.org/10.1210/ENDOCR/BQAA106.

Gilbert, M.E., O'Shaughnessy, K.L., Thomas, S.E., Riutta, C., Wood, C.R., Smith, A., Oshiro, W.O., Ford, R.L., Hotchkiss, M.G., Hassan, I., Ford, J.L., 2021. Thyroid disruptors: extrathyroidal sites of chemical action and neurodevelopmental outcome—an examination using triclosan and perfluorohexane sulfonate. Toxicol. Sci. 183, 195–213. https://doi.org/10.1093/TOXSCI/KFAB080.

Goldey, E.S., Kehn, L.S., Rehnberg, G.L., Crofton, K.M., 1995. Effects of developmental hypothyroidism on auditory and motor function in the rat. Toxicol. Appl. Pharmacol. 135, 67–76. https://doi.org/10.1006/TAAP.1995.1209.

Hamers, T., Kamstra, J.H., Sonneveld, E., Murk, A.J., Kester, M.H.A., Andersson, P.L., Legler, J., Brouwer, A., 2006. In vitro profiling of the endocrine-disrupting potency of brominated flame retardants. Toxicol. Sci. 92, 157–173. https://doi.org/10.1093/TOXSCI/KFJ187.

Hansen, M., Luong, X., Sedlak, D.L., Helbing, C.C., Hayes, T., 2016. Quantification of 11 thyroid hormones and associated metabolites in blood using isotope-dilution liquid chromatography tandem mass spectrometry. Anal. Bioanal. Chem. 408, 5429–5442. https://doi.org/10.1007/S00216-016-9614-9.

Hrabovszky, E., Wittmann, G., Turi, G.F., Liposits, Z., Fekete, C., 2005. Hypophysiotropic thyrotropin-releasing hormone and corticotropin-releasing hormone neurons of the rat contain vesicular glutamate Transporter-2. Endocrinology 146, 341–347. https://doi.org/10.1210/EN.2004-0856.

Huang, J., Guo, L., 2017. Knockdown of SOX9 inhibits the proliferation, invasion, and EMT in thyroid cancer cells. Oncol. Res. 25, 167. https://doi.org/10.3727/096504016X14732772150307.

Johnson, J., Gibson, S., Ober, R., 1984. Cholestyramine-enhanced fecal elimination of carbon-14 in rats after administration of ammonium [14C]perfluorooctanoate or potassium [14C]perfluorooctanesulfonate. Fund. Appl. Toxicol. 4, 972–976. https://doi.org/10.1016/0272-0590(84)90235-5.

Kim, S., Webster, M.J., 2010. Integrative genome-wide association analysis of cytoarchitectural abnormalities in the prefrontal cortex of psychiatric disorders, 2011 Mol. Psychiatr. 164 (16), 452–461. https://doi.org/10.1038/mp.2010.23.

Klaassen, C.D., Hood, A.M., 2001. Effects of microsomal enzyme inducers on thyroid follicular cell proliferation and thyroid hormone metabolism. Toxicol. Pathol. 29, 34–40. https://doi.org/10.1080/019262301301418838.

Kodavanti, P.R.S., Coburn, C.G., Moser, V.C., MacPhail, R.C., Fenton, S.E., Stoker, T.E., Rayner, J.L., Kannan, K., Birnbaum, L.S., 2010. Developmental exposure to a commercial PBDE mixture, DE-71: neurobehavioral, hormonal, and reproductive effects. Toxicol. Sci. 116, 297–312. https://doi.org/10.1093/TOXSCI/KFQ105.

Lau, C., Thibodeaux, J.R., Hanson, R.G., Rogers, J.M., Grey, B.E., Stanton, M.E., Buttenhoff, J.L., Stevenson, L.A., 2003. Exposure to perfluorooctane sulfonate during pregnancy in rat and mouse. II: postnatal evaluation. Toxicol. Sci. https://doi.org/10.1093/toxsci/kfg122.

Lee, J.E., Choi, K., 2017. Perfluoroalkyl substances exposure and thyroid hormones in humans: epidemiological observations and implications. Ann. Pediatr. Endocrinol. Metab. 22, 6. https://doi.org/10.6065/APEM.2017.22.1.6.

Li, J., Liu, B., Chen, C., Cui, Y., Shang, L., Zhang, Y., Wang, C., Zhang, X., He, Q., Zhang, W., Bi, W., Jiang, T., 2015. RAB2A Polymorphism impacts prefrontal morphology, functional connectivity, and working memory. Hum. Brain Mapp. 36, 4372. https://doi.org/10.1002/HBM.22924.

Liu, J., Liu, Y., Barter, R.A., Klaassen, C.D., 1995. Alteration of thyroid homeostasis by UDP-glucuronosyltransferase inducers in rats: a dose-response study. J. Pharmacol. Exp. Therapeut. 273.

Louis, G.W., Hallinger, D.R., Braxton, M.J., Kamel, A., Stoker, T.E., 2017. Effects of chronic exposure to triclosan on reproductive and thyroid endpoints in the adult Wistar female rat. J. Toxicol. Environ. Health 80, 236. https://doi.org/10.1080/15287394.2017.1287029.

Love, M.I., Huber, W., Anders, S., 2014. Moderated estimation of fold change and dispersion for RNA-seq data with DESeq2. Genome Biol. 15, 1–21. https://doi.org/10.1186/S13059-014-0550-8/FIGURES/9.

Luebker, D.J., York, R.G., Hansen, K.J., Moore, J.A., Butenhoff, J.L., 2005. Neonatal mortality from in utero exposure to perfluorooctanesulfonate (PFOS) in Sprague–Dawley rats: dose–response, and biochemical and pharamacokinetic parameters. Toxicology 215, 149–169. https://doi.org/10.1016/J.TOX.2005.07.019.

Luo, W., Brouwer, C., 2013. Pathview: an R/Bioconductor package for pathway-based data integration and visualization. Bioinformatics 29, 1830–1831. https://doi.org/10.1093/BIOINFORMATICS/BTT285.

Merchenthaler, I., Liposits, Z., 1994. Mapping of thyrotropin-releasing hormone (TRH) neuronal systems of rat forebrain projecting to the median eminence and the OVLT. Immunocytochemistry combined with retrograde labeling at the light and electron microscopic levels. Acta Biol. Hung. 45, 361–374.

Morita, A., Yamashita, N., Sasaki, Y., Uchida, Y., Nakajima, O., Nakamura, F., Yagi, T., Taniguchi, M., Usui, H., Katoh-Semba, R., Takei, K., Goshima, Y., 2006. Regulation of dendritic branching and spine maturation by Semaphorin3A-Fyn signaling. J. Neurosci. 26, 2971. https://doi.org/10.1523/JNEUROSCI.5453-05.2006.

Olsen, G.W., Burris, J.M., Ehresman, D.J., Froelich, J.W., Seacat, A.M., Butenhoff, J.L., Zobel, L.R., 2007. Half-life of serum elimination of perfluorooctanesulfonate, perfluorohexanesulfonate, and perfluorooctanoate in retired fluorochemical production workers. Environ. Health Perspect. 115, 1298–1305. https://doi.org/10.1289/EHP.10009.

Pasterkamp, R.J., Giger, R.J., 2009. Semaphorin function in neural plasticity and disease. Curr. Opin. Neurobiol. 19, 263. https://doi.org/10.1016/J.CONB.2009.06.001.

Ramhøj, L., Hass, U., Boberg, J., Scholze, M., Christiansen, S., Nielsen, F., Axelstad, M., 2018. Perfluorohexane sulfonate (PFHxS) and a mixture of endocrine disrupters reduce thyroxine levels and cause antiandrogenic effects in rats. Toxicol. Sci. 163, 579–591. https://doi.org/10.1093/TOXSCI/KFY055.

Ramhøj, L., Hass, U., Gilbert, M.E., Wood, C., Svingen, T., Usai, D., Vinggaard, A.M., Mandrup, K., Axelstad, M., 2020. Evaluating thyroid hormone disruption: investigations of long-term neurodevelopmental effects in rats after perinatal exposure to perfluorohexane sulfonate (PFHxS). Sci. Rep. 10 https://doi.org/10.1038/S41598-020-59354-Z.

Rao, S., Kupfer, Y., Pagala, M., Chapnick, E., Tessler, S., 2011. Systemic absorption of oral vancomycin in patients with Clostridium difficile infection. Scand. J. Infect. Dis. 43, 386–388. https://doi.org/10.3109/00365548.2010.544671.

Ren, X.M., Qin, W.P., Cao, L.Y., Zhang, J., Yang, Y., Wan, B., Guo, L.H., 2016. Binding interactions of perfluoroalkyl substances with thyroid hormone transport proteins and potential toxicological implications. Toxicology 366 (367), 32–42. https://doi.org/10.1016/J.TOX.2016.08.011.

Ritchie, M.E., Phipson, B., Wu, D., Hu, Y., Law, C.W., Shi, W., Smyth, G.K., 2015. Limma powers differential expression analyses for RNA-sequencing and microarray studies. Nucleic Acids Res. 43, e47. https://doi.org/10.1093/NAR/GKV007.

Rosen, M.B., Das, K.P., Rooney, J., Abbott, B., Lau, C., Corton, J.C., 2017. PPARα-independent transcriptional targets of perfluoroalkyl acids revealed by transcript profiling. Toxicology 387, 95–107. https://doi.org/10.1016/J.TOX.2017.05.013.

Rosen, M.B., Lee, J.S., Ren, H., Vallanat, B., Liu, J., Waalkes, M.P., Abbott, B.D., Lau, C., Corton, J.C., 2008. Toxicogenomic dissection of the perfluorooctanoic acid transcript profile in mouse liver: evidence for the involvement of nuclear receptors PPARα and CAR. Toxicol. Sci. 103, 46–56. https://doi.org/10.1093/TOXSCI/KFN025.

Rosen, M.B., Schmid, J.R., Corton, J.C., Zehr, R.D., Das, K.P., Abbott, B.D., Lau, C., 2010. Gene expression profiling in wild-type and PPARα-null mice exposed to perfluorooctane sulfonate reveals PPARα-independent effects. PPAR Res. 2010 https://doi.org/10.1155/2010/794739.

Rosenmai, A.K., Ahrens, L., le Godec, T., Lundqvist, J., Oskarsson, A., 2018. Relationship between peroxisome proliferator-activated receptor alpha activity and cellular concentration of 14 perfluoroalkyl substances in HepG2 cells. J. Appl. Toxicol. 38 https://doi.org/10.1002/jat.3515.

Rudolf, R., Bittins, C.M., Gerdes, H.H., 2011. The role of myosin V in exocytosis and synaptic plasticity. J. Neurochem. 116, 177–191. https://doi.org/10.1111/J.1471-4159.2010.07110.X.

Salgado, R., López-Doval, S., Pereiro, N., Lafuente, A., 2016. Perfluorooctane sulfonate (PFOS) exposure could modify the dopaminergic system in several limbic brain regions. Toxicol. Lett. 240, 226–235. https://doi.org/10.1016/J.TOXLET.2015.10.023.

Salgado, R., Pereiro, N., López-Doval, S., Lafuente, A., 2015. Initial study on the possible mechanisms involved in the effects of high doses of perfluorooctane sulfonate (PFOS) on prolactin secretion. Food Chem. Toxicol. 83, 10–16. https://doi.org/10.1016/j.fct.2015.05.013.

Schrenk, D., Bignami, M., Bodin, L., Chipman, J.K., del Mazo, J., Grasl-Kraupp, B., Hogstrand, C., Hoogenboom, L., Leblanc, J.C., Nebbia, C.S., Nielsen, E., Ntzani, E., Petersen, A., Sand, S., Vleminckx, C., Wallace, H., Barregård, L., Ceccatelli, S., Cravedi, J.P., Halldorsson, T.I., Haug, L.S., Johansson, N., Knutsen, H.K., Rose, M., Roudot, A.C., Van Loveren, H., Vollmer, G., Mackay, K., Riolo, F., Schwerdtle, T., 2020. Risk to human health related to the presence of perfluoroalkyl substances in food. EFSA J. 18 https://doi.org/10.2903/j.efsa.2020.6223.

Seacat, A.M., Thomford, P.J., Hansen, K.J., Olsen, G.W., Case, M.T., Butenhoff, J.L., 2002. Subchronic toxicity studies on perfluorooctanesulfonate potassium salt in cynomolgus monkeys. Toxicol. Sci. 68, 249–264. https://doi.org/10.1093/TOXSCI/68.1.249.

Smyth, G.K., 2004. Linear models and empirical bayes methods for assessing differential expression in microarray experiments. Stat. Appl. Genet. Mol. Biol. 3 https://doi.org/10.2202/1544-6115.1027/MACHINEREADABLECITATION/RIS.

Steinfelder, H.J., Hauser, P., Nakayama, Y., Radovick, S., Mcclaskey, J.H., Taylor, T., Weintraub, B.D., Wondisford, F.E., 1991. Thyrotropin-releasing hormone regulation of human TSHB expression: role of a pituitary-specific transcription factor (Pit-1/GHF-1) and potential interaction with a thyroid hormone-inhibitory element. Proc. Natl. Acad. Sci. U. S. A 88, 3130–3134. https://doi.org/10.1073/PNAS.88.8.3130.

Sunderland, E.M., Hu, X.C., Dassuncao, C., Tokranov, A.K., Wagner, C.C., Allen, J.G., 2019. A review of the pathways of human exposure to poly- and perfluoroalkyl substances (PFASs) and present understanding of health effects. J. Expo. Sci. Environ. Epidemiol. 29, 131. https://doi.org/10.1038/S41370-018-0094-1.

Takacs, M.L., Abbott, B.D., 2007. Activation of mouse and human peroxisome proliferator-activated receptors (alpha, beta/delta, gamma) by perfluorooctanoic acid and perfluorooctane sulfonate. Toxicol. Sci. 95, 108–117. https://doi.org/10.1093/TOXSCI/KFL135.

Thibodeaux, J.R., Hanson, R.G., Rogers, J.M., Grey, B.E., Barbee, B.D., Richards, J.H., Butenhoff, J.L., Stevenson, L.A., Lau, C., 2003. Exposure to perfluorooctane sulfonate during pregnancy in rat and mouse. I: maternal and prenatal evaluations. Toxicol. Sci. 74, 369–381. https://doi.org/10.1093/TOXSCI/KFG121.

UNEP, 2008. Overview [WWW document]. URLaccessed 1.28.21. http://chm.pops.int/Implementation/IndustrialPOPs/PFOS/Overview/tabid/5221/Default.aspx.

van der Spek, A.H., Fliers, E., Boelen, A., 2017. The classic pathways of thyroid hormone metabolism. Mol. Cell. Endocrinol. 458, 29–38. https://doi.org/10.1016/J.MCE.2017.01.025.

Wang, Q., Shen, Y., Ye, B., Hu, H., Fan, C., Wang, T., Zheng, Y., Lv, J., Ma, Y., Xiang, M., 2018. Gene expression differences between thyroid carcinoma, thyroid adenoma and normal thyroid tissue. Oncol. Rep. 40, 3359. https://doi.org/10.3892/OR.2018.6717.

Wang, Y., Wang, L., Chang, W., Zhang, Yinfeng, Zhang, Yuan, Liu, W., 2019. Neurotoxic effects of perfluoroalkyl acids: neurobehavioral deficit and its molecular mechanism. Toxicol. Lett. 305, 65–72. https://doi.org/10.1016/J.TOXLET.2019.01.012.

Weiss, J.M., Andersson, P.L., Lamoree, M.H., Leonards, P.E.G., Van Leeuwen, S.P.J., Hamers, T., 2009. Competitive binding of poly- and perfluorinated compounds to the thyroid hormone transport protein transthyretin. Toxicol. Sci. 109, 206–216. https://doi.org/10.1093/TOXSCI/KFP055.

Wolf, C.J., Takacs, M.L., Schmid, J.E., Lau, C., Abbott, B.D., 2008. Activation of mouse and human peroxisome proliferator-activated receptor alpha by perfluoroalkyl acids of different functional groups and chain lengths. Toxicol. Sci. 106, 162–171. https://doi.org/10.1093/TOXSCI/KFN166.

Yang, R., Liu, S., Liang, X., Yin, N., Ruan, T., Jiang, L., Faiola, F., 2020. F–53B and PFOS treatments skew human embryonic stem cell in vitro cardiac differentiation towards epicardial cells by partly disrupting the WNT signaling pathway. Environ. Pollut. 261, 114153. https://doi.org/10.1016/j.envpol.2020.114153.

Yang, Y.R., Kang, D.S., Lee, C., Seok, H., Follo, M.Y., Cocco, L., Suh, P.G., 2016. Primary phospholipase C and brain disorders. Adv. Biol. Regul. 61, 80–85. https://doi.org/10.1016/J.JBIOR.2015.11.003.

Yin, W., Sun, Z., Mendenhall, J.M., Walker, D.M., Riha, P.D., Bezner, K.S., Gore, A.C., 2015. Expression of vesicular glutamate transporter 2 (vGluT2) on large dense-core vesicles within GnRH neuroterminals of aging female rats. PLoS One 10, e0129633. https://doi.org/10.1371/JOURNAL.PONE.0129633.

Yoshida, Y., 2012. Semaphorin signaling in vertebrate neural circuit assembly. Front. Mol. Neurosci. 5 https://doi.org/10.3389/FNMOL.2012.00071.

Yu, W.G., Liu, W., Jin, Y.-H., Liu, X.H., Wang, F.Q., Liu, L., Nakayama, S.F., 2009. Prenatal and postnatal impact of perfluorooctane sulfonate (PFOS) on rat development: a cross-foster study on chemical burden and thyroid hormone system. Environ. Sci. Technol. 43, 8416–8422. https://doi.org/10.1021/ES901602D.

Yu, W.G., Liu, W., Jin, Y.H., 2009. Effects of perfluorooctane sulfonate on rat thyroid hormone biosynthesis and metabolism. Environ. Toxicol. Chem. 28, 990–996. https://doi.org/10.1897/08-345.1.

Zhao, W., Zitzow, J.D., Weaver, Y., Ehresman, D.J., Chang, S.-C., Butenhoff, J.L., Hagenbuch, B., 2017. Organic anion transporting polypeptides contribute to the disposition of perfluoroalkyl acids in humans and rats. Toxicol. Sci. 156, 84–95. https://doi.org/10.1093/TOXSCI/KFW236.